JOURNAL OF CATALYSIS 45, 86–93 (1976)

Kinetics of Oxidation of Cumene over Supported NiO and $NiMoO_4$ Catalysts

A. K. AGARWAL AND R. D. SRIVASTAVA[1]

Department of Chemical Engineering, Indian Institute of Technology, Kanpur 208016, India

Received February 13, 1976

Kinetics and catalytic behavior of NiO supported on alumina and on activated carbon and $NiMoO_4$ supported on alumina have been studied in the liquid phase oxidation of cumene. The catalysts have been characterized by means of DTA, TGA, X-ray, ir, and BET studies. Detailed studies of the concentration of main products of cumene along with the effect of catalyst weight, and hydrocarbon concentration on the rate of oxidation were conducted at 80°C employing these supported catalysts. A reaction mechanism is proposed in which the catalyst plays an important role in the initiation and termination steps. Rate equations derived are in good agreement with the experimental data. It was observed that carbon as a support relative to alumina (NiO catalysts) induced increased activity, lower activation energies, and shifted the limiting oxidation rate to lower catalyst amounts.

INTRODUCTION

The oxidation of cumene has been the subject of numerous investigations in the past, thus making it difficult to give a comprehensive review of this reaction. Moreover, there are only few cases (1–6) among the variety of catalysts studied wherein significant attention has been given to the insoluble catalysts and the heterogeneous reactions. The kinetics and catalytic behavior of oxidation of cumene in the presence of supported nickel oxide and supported $NiMoO_4$ have not been discussed in the literature.

A number of authors (*7–11*) has treated in some detail the solid state properties of alumina-supported nickel oxide and nickel molybdate; however, very little is reported of the characterization of nickel oxide on activated carbon (*12*).

Presented in this paper are the results of oxidation of cumene over $NiO–Al_2O_3$, NiO–C, and $NiMoO_4–Al_2O_3$ catalysts coupled with the characterization of these catalysts by means of DTA, TGA, X-ray, ir, and BET studies. In this investigation, we limit ourselves to present results on the commercial catalysts.

The principal purpose of this study is to examine the effect of several variables, catalyst weight, hydrocarbon concentration, and reaction temperature along with the concentrations of the main products of oxidation as influenced by nickel oxide on different supports. Experimental data of this type are expected to lead to a better understanding of a degenerate chain-branching mechanism and, especially to evaluate the role of the catalyst and support in such reaction. In addition, physicochemical characterization is desired in order to amplify literature results for these systems.

EXPERIMENTAL

Materials

Nickel oxide supported on activated carbon (22% NiO) and on alumina (65%

[1] Author to whom correspondence should be addressed.

NiO), and nickel molybdate supported on alumina (5% NiO, 10% MoO_3), were supplied by Girdler Company. The catalysts were crushed and screened to 150 mesh. Pure nickel oxide was obtained from Fisher Scientific in the powdered form. Reference to the various samples will be made as NiO or $NiMoO_4$ followed by the support.

Cumene obtained from Herdillia Chemicals was fractionally distilled. This was treated with concentrated sulfuric acid followed by dilute alkali and washed with distilled water. The dried cumene was stored in a nitrogen atmosphere.

Chlorobenzene obtained from Sarabhai Chemicals was washed with concentrated sulfuric acid, washed with distilled water, and dried before use. Cumene hydroperoxide was prepared by the thermal oxidation of cumene using MnO_2 as a catalyst at 60°C.

PHYSICOCHEMICAL CHARACTERIZATION

No extensive determinations have been published on the physical properties and characteristics of these particular catalysts.

X-Ray

The X-ray diffraction patterns were recorded using a General Electronics diffractometer (XRD-VI Generator, SPG-4 detector, and SPG-2 diffractometer) with copper ($K\alpha$) radiation. The diffractometer was operated with 2° diverging and receiving slits at a scan rate of 1°/min and a continuous trace of intensity as a function of 2θ was recorded. The accuracy of Bragg's angle positions were checked using a permaquartz standard sample. Spectra of finely ground samples were run in the 2θ range 5–80°.

X-ray powder diffraction of $NiO–Al_2O_3$ samples showed the presence of crystalline NiO (ASTM4-0835). In the NiO–C samples broad diffraction bands of NiO were found which were attributed to low concentration of nickel oxide in the support. The intensity of the line at d = 2.08 Å increased in the $NiO–Al_2O_3$ catalysts as compared with the NiO–C catalysts.

XRD study of $NiMoO_4–Al_2O_3$ samples showed the presence of alumina and absence of characteristic diffraction bands of the Ni–Mo–O system. The spectra of the alumina samples were similar to Stumpf and co-workers (*13*) alumina.

DTA and TGA

DTA measurements were carried out on a Dupont-900 apparatus equipped with high temperature cell, using calibrated platinum/platinum–13% rhodium thermocouples. TGA was performed by Aminco Modular Thermo-Grav. apparatus, with programmed temperature increase, under atmospheric conditions. TGA measurements were carried out by heating the samples at a rate of 10°C/min.

A programmed heating at a rate of 12°C/min between 25 and 1000°C was used in DTA measurements. The analysis of an NiO–C sample showed an endothermal transformation at 116°C, followed by an exothermal drift at about 466°C; no further transformation was observed. The exothermal transformation at 466°C can be explained as due to burning of carbon. This is in agreement with the observation that the TGA curve at this temperature showed a rapid loss in the weight. In the case of $NiO–Al_2O_3$ system, only one small effect was observed: endothermic at about 300°C. Indeed the TGA curve also showed a weight loss between 120 to 400°C. However, this loss is only small (of the order 2%). The endothermal trends for both catalysts probably simply result from dehydrations.

In the case of $NiMoO_4–Al_2O_3$ system, TGA curve also showed a weight loss starting from 100°C. DTA of an $NiMoO_4–Al_2O_3$ sample showed the endothermal effects, a broad effect from 100 to 300°C and a very small at 690°C. A similar effect at 690°C was observed while studying the structure

TABLE 1

Physical Characteristics of Catalysts

Catalyst	Surface area (m^2/g)	Pore volume[a] (cm^3/g)	Mean pore radius (Å)
$NiO–Al_2O_3$	24	0.37	311
NiO–C	243	0.57	47
$NiMoO_4–Al_2O_3$	48	0.12	50

[a] Referred to 1500 atm.

of $NiMoO_4$ (*14*). This was attributed to a structural transformation from α- to β-$NiMoO_4$. This transformation is in agreement with the observation that TGA curve at this temperature became more flat.

Infrared Spectroscopy

Transmittance spectra for powdered samples (<150 mesh) were recorded on a Perkin–Elmer-521 Grating ir spectrophotometer using KBr disk.

In the transmittance spectra of $NiO–Al_2O_3$ system (65 wt% NiO), we noticed the intense absorption of NiO (plateau in the 800–400 cm^{-1} region) covering any diagnostic Al–O frequency in the bulk. The 900 cm^{-1} Al–O (plateau in the 940–500 cm^{-1} region) resolved into a set of components at 925 and 885, which is attributable to free Al_2O_3 present in the bulk.

In the NiO–C (22 wt% NiO) system the transmittance spectra show absorptions at 650 and 400 cm^{-1}, which are attributable to free NiO present in the bulk.

The spectra of $NiMoO_4–Al_2O_3$ samples showed the intense absorption of Al_2O_3 (plateau in the 940–500 cm^{-1} region) covering any diagnostic Ni–Mo–O frequency of the bulk.

The transmittance spectra of Al_2O_3 and NiO samples were similar to previously reported spectra of these oxides (*15*, *16*).

Surface Area and Pore Volume

Surface areas of powdered catalysts were calculated from N_2 adsorption isotherms using BET apparatus. Pore volume and pore size distribution were measured by a mercury porosimeter Carlo-Erba Model-70 for the 2000 atm range.

Surface area (SA), pore volume (V_p), and calculated pore radii ($r = 2V_p/SA$) for the three supported catalysts are given in Table 1. Catalyst $NiO–Al_2O_3$ is characterized by a low pore volume and small surface area, which results in a higher value of mean pore radii.

Oxidation Apparatus

The oxidation apparatus and technical procedure have been described previously (*1*). The products of oxidation were analyzed by titration as well with a Perkin–Elmer, Model 137 ir spectrophotometer. The experiments were conducted at a temperature of 80°C.

RESULTS AND DISCUSSION

From the earlier experiments (*1*), it was concluded that addition of both the catalyst (M) and hydroperoxide (ROOH) was necessary to initiate the oxidation of cumene. There existed a limited value of initial hydroperoxide concentration below which the oxidation was negligible. Beyond this limiting value, there was no effect of increase in hydroperoxide concentration on the oxygen absorption rate. These were also evident in the present study.

A critical ratio of hydroperoxide concentration to catalyst amount of approximately $3–4 \times 10^{-4}$ g mole/g of catalyst was obtained for all the catalysts. Further runs on cumene oxidation were conducted with this ratio.

Figure 1 shows the oxygen consumption against time for a fixed amount of NiO. The amount of NiO–C and $NiO–Al_2O_3$ catalysts corresponding to 0.01 g of NiO was used. Also, included in the plot are the oxidation curves for systems containing the support materials, i.e., Al_2O_3 and carbon with hydroperoxide initiator. The results

obtained for NiO are similar to those of Varma and Graydon (*2*). Considerable differences in catalyst performance are quite evident from an examination of this plot.

Immediately apparent from the oxygen consumption plots of Fig. 1 is an observable effect; a clear distinction of relative reactivity for this reaction among the catalysts tested is evident, the reactivity being judged by the oxygen consumption at the equal contact time, temperature, and fixed catalyst amount. In spite of the NiO percentage not being the same in NiO–C and NiO–Al_2O_3 systems, the general results indicate a pattern which can be used to characterize these metal oxide catalysts with respect to the type of support. These reactivities may be summarized by the following sequence:

$$NiO\text{–}C > NiO\text{–}Al_2O_3 > NiO.$$

Influence of Catalyst Weight and Hydrocarbon Concentration

Reaction orders with respect to the catalyst amount were determined from the slopes of the curves shown in Fig. 2, considering all points at catalyst ratios below the apparent change in mechanism as indicated by the break in the curve. The values obtained are presented in Table 2.

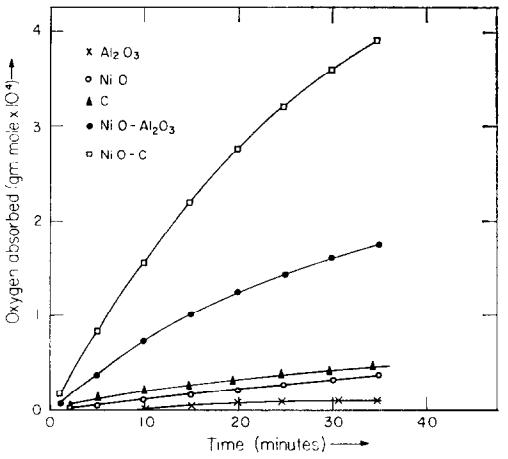

FIG. 1. Oxygen adsorption curves for 1 ml of cumene at 80°C for difference catalysts. Amount of catalysts corresponding to 0.01 g of NiO was used.

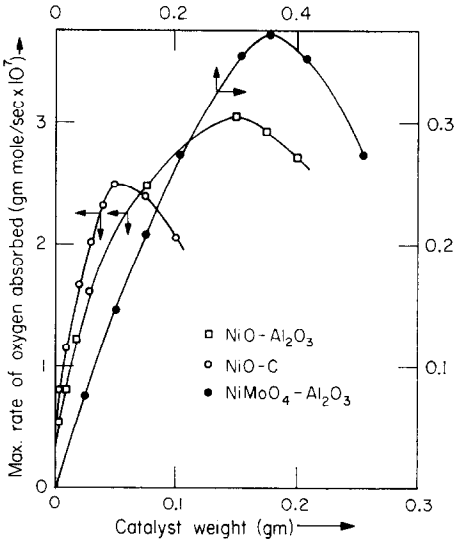

FIG. 2. Measured rates of oxygen absorption for 1 ml of cumene at 80°C as a function of catalyst weights.

Meyer *et al.* (*17*) and Neuberg *et al.* (*18*) obtained apparent order of 0.70 and 0.63 with MnO_2 catalyst, in the liquid phase oxidation of cyclohexene. This type of deviation from a theoretical value of 0.5 has been reported by other authors (*1*, *19*) and, of course, is evident in the present study of $NiMoO_4$–Al_2O_3 catalyzed runs.

The influence of hydrocarbon concentration on the rate of oxidation was studied with mixtures of cumene and monochlorobenzene, employing NiO–C, NiO–Al_2O_3, and $NiMoO_4$–Al_2O_3 as catalysts. Runs were made at a catalyst ratio of 0.03 g/ml for all the catalysts. This ratio was chosen on the basis that in this region of catalyst ratios and hydrocarbon concentrations, the

TABLE 2

Catalyst	Catalyst order	Hydrocarbon order	Activation energy (kcal/mole)
NiO–Al_2O_3	0.5	1.2	16.0
NiO–C	0.5	1.1	12.3
$NiMoO_4$–Al_2O_3	0.8	1.2	—

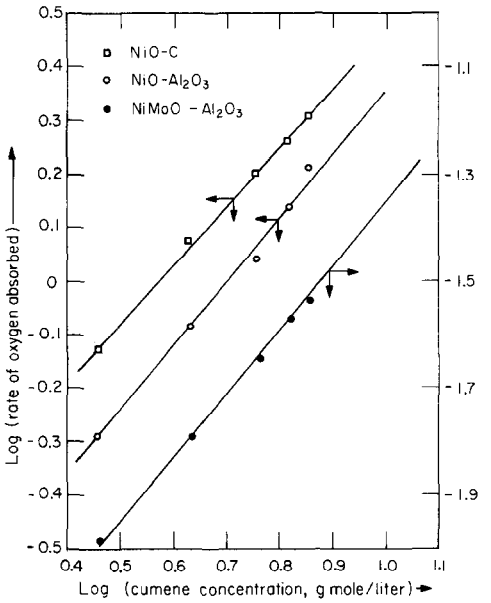

FIG. 3. Rate dependence with respect to cumene concentration for different catalysts at 80°C.

limiting rate of oxidation was not attained (*20*).

In Fig. 3, the logarithmic rates of oxygen absorption are plotted against hydrocarbon concentrations. The orders are summarized in Table 2.

When the initiation is of first order with respect to catalyst and termination bi-radical, and an overall order of 0.5 will be obtained. The present results clearly confirm the idea of heterogeneous initiation and homogeneous terminations of the chains.

As shown in Fig. 2, the catalyst NiO–Al_2O_3, low specific surface (Table 1), the oxidation rate declined for catalyst ratios over 150 mg/ml. A similar retarding effect was observed for $NiMoO_4$–Al_2O_3 catalyst. The curve corresponding to NiO–C catalyst, high specific surface (Table 1), shows that for catalyst ratios over 50 mg/ml the rates are markedly depressed. Tobolsky *et al.* (*21*) have suggested that the initiation of free radicals in metal catalyzed oxidations is due to degenerate chain branching and when the rates of formation and decomposition of hydroperoxide in the solution become equal, hydroperoxide reaches a stationary concentration whereupon a limiting oxidation is reached. The retarding effect of the catalyst may arise from the secondary termination of peroxy radicals on the surface of the solid.

The decrease in rate after the maximum was also observed by Srivastava and Srivastava (*1*) and Varma and Graydon (*2*), where the oxidation of cumene was studied with transition metal oxides. Their rate of oxidation after the maximum dropped catastrophically. In the present work such a sharp decay was not observed. The occurrence of relatively long decay in the presence of large quantities of support is believed to be caused by physical adsorption of peroxy radicals.

Product Distribution

Another important reaction characteristic, that of product distribution, was also obtained from these studies. These distributions as a function of catalyst weight (for supported NiO catalysts) are presented in Table 3. One property of the product distribution results, however, is quite clear. In both the catalysts, before the limiting rate conditions, as the catalyst weight was increased, the mole% yield of hydroperoxide increased. Near and after the break in point, hydroperoxide in the total oxidized products decreased as the catalyst was increased, while the percentage of cumyl alcohol and acetophenone seems to increase.

In the case of $NiMoO_4$–Al_2O_3 system, the concentration of cumyl alcohol was much greater than the concentration of acetophenone when the lower weight of the catalyst was employed. In fact, the production of acetophenone was negligible at low catalyst ratios. At higher catalyst ratios, the molar concentration of alcohol and ketone produced were the same.

TABLE 3

Distribution of Products of Cumene Oxidation with NiO–C and NiO–Al_2O_3 Catalysts[a]

Catalyst wt (g)	NiO–C			NiO–Al_2O_3		
	Hydroperoxide	Alcohol	Ketone	Hydroperoxide	Alcohol	Ketone
0.005	63.6	36.4	—[b]	41.1	58.9	—[b]
0.01	68.7	31.3	—[b]	54.0	37.2	8.8
0.05	59.7	34.7	5.6	58.5	27.4	14.1
0.1	46.4	34.6	19.0	46.6	30.6	22.8
0.2				38.2	31.3	30.5

[a] All the concentrations are reported in mole%. Amount of initial hydroperoxide is included in the hydroperoxide concentration. Reaction temperature, 80°C; volume of cumene, 1 ml; reaction time 30 min.

[b] Acetophenone was detectable in infrared spectra but the intensity of absorption was too small for accurate measurements.

Reaction Mechanism

The purpose of this work was to consider a mechanism which would be consistent with the following observations:

(a) For low catalyst ratios, the apparent orders of the reaction with respect to catalyst weight and the hydrocarbon concentration are 0.5 and 1.0, respectively;

(b) There is a critical weight of the catalysts above which the rate of oxidation drops sharply;

(c) There is a critical hydroperoxide to catalyst ratio below which the oxidation was negligible;

(d) An excess of initial hydroperoxide does not affect the reaction rate; and

(e) For a fixed cumene concentration and increasing catalyst ratios, the rate of hydroperoxide increases, passing through a maximum, and then decreases with catalyst.

The following mechanism is an adaptation of that recently proposed by Neuberg *et al.* (*18*) to explain the kinetics of oxidation of cyclohexene.

Initiation:

$$\mathrm{ROOH} + \mathrm{M} \overset{K_1}{\rightleftarrows} (\mathrm{ROOH}\ldots\mathrm{M}) \quad (1)$$

$$(\mathrm{ROOH}\ldots\mathrm{M}) \xrightarrow{k_2} \mathrm{RO}\cdot + \cdot\mathrm{OH}\ldots\mathrm{M} \quad (2)$$

$$\mathrm{ROOH} + \cdot\mathrm{OH}\ldots\mathrm{M} \xrightarrow{k_3} \mathrm{RO_2}\cdot + \mathrm{H_2O} + \mathrm{M} \quad (3)$$

$$\mathrm{RO}\cdot + \mathrm{RH} \xrightarrow{k_4} \mathrm{ROH} + \mathrm{R}\cdot \quad (4)$$

Propagation:

$$\mathrm{R}\cdot + \mathrm{O_2} \xrightarrow{k_5} \mathrm{RO_2}\cdot \quad (5)$$

$$\mathrm{RO_2}\cdot + \mathrm{RH} \xrightarrow{k_6} \mathrm{ROOH} + \mathrm{R}\cdot \quad (6)$$

Termination:

$$\mathrm{RO_2}\cdot + \mathrm{RO_2}\cdot \xrightarrow{k_7} \text{Inactive products} + \mathrm{O_2} \quad (7)$$

$$\mathrm{RO_2}\cdot + \mathrm{M} \overset{K_8}{\rightleftarrows} (\mathrm{RO_2}\cdot\ldots\mathrm{M}) \quad (8)$$

$$\mathrm{RO_2}\cdot + (\mathrm{RO_2}\cdot\ldots\mathrm{M}) \xrightarrow{k_9} \text{Inactive products.} \quad (9)$$

If oxygen evolved from the biradical termination is neglected with respect to oxygen absorbed in the propagation, the general rate of oxidation can be expressed as

$$-\frac{d[\mathrm{O_2}]}{dt} = k_6\left(\frac{R_i}{2k_7 + K_8k_9[\mathrm{M}]}\right)^{\frac{1}{2}}[\mathrm{RH}] \quad (10)$$

where R_i is the rate of free radical initiation.

If the termination rate of peroxy radicals on the catalyst surface (Eqs. 8 and 9) is negligible compared with the biradical ter-

mination rate (Eq. 7), then the rate of oxidation will be given by

$$-\frac{d[O_2]}{dt} = k_6\left(\frac{R_i}{2k_7}\right)^{\frac{1}{2}}[RH]. \quad (11)$$

It may be assumed that R_i is proportional to the amount of catalyst. Comparing with the apparent order values in Table 2, it is observed that Eq. 11 explains well the NiO–C, $NiO–Al_2O_3$, and $NiMoO_4–Al_2O_3$ catalyzed runs.

A second rate expression can be derived in the case where a limiting oxidation is reached. The derivation is similar to one proposed by Neuberg *et al.* (*18*). Under limiting condition, the rate of formation of hydroperoxide through reaction (6) becomes equal to the rate of decomposition on the catalyst surface, R_d. The total rate of formation of hydroperoxide is simply

$$\frac{d[ROOH]}{dt} = k_6\left(\frac{R_i}{2k_7 + K_8k_9[M]}\right)^{\frac{1}{2}}[RH] - R_d \equiv 0. \quad (12)$$

Let $R_i = \alpha R_d$, where α is the fraction of hydroperoxide decomposed yielding free radicals. For a small value of α, the limiting rate of oxidation is given by

$$-\left(\frac{d[O_2]}{dt}\right) = \frac{\alpha k_6^2[RH]^2}{2k_7 + K_8k_9[M]}. \quad (13)$$

It is very clear from Eq. 13 that for high catalyst ratios a point must be reached where $K_8k_9[M] \gg 2k_7$ and inhibition will start to be effective. It also explains the behavior of NiO–C catalyst (high active sites) where a limiting rate at a much lower catalyst ratio was observed.

Under limiting rate condition, the apparent order with respect to hydrocarbon concentration is derived as 2. It is well known that the rate of oxygen consumption may present different reaction orders with respect to hydrocarbon concentration, depending upon the conditions of oxidation. Kamiya *et al.* (*20*) and Neuberg *et al.* (*18*) have shown that if the oxidation proceeds via a chain branching mechanism and the limiting rate has been attained, the reaction order will lie above 1.

Activation Energy

Lastly, we note in Table 2 that the activation energies are lower for nickel oxide when supported on carbon compared with alumina-supported nickel oxide. The effect of temperature on reaction rate was studied in the range of 70–80°C. Generally, carbon as a support relative to alumina induces increased catalytic activity, lowers activation energies, and shifts the limiting oxidation rate to lower catalyst amounts. Some of these conclusions are in the line with the interpretation proposed by Schwab (*22*).

From the present results we conclude that the catalytic activities of supported NiO and supported $NiMoO_4$ are mainly due to capability of decomposing hydroperoxides into the chain-initiating radicals. The oxidation of cumene proceed via a degenerate chain branching mechanism.

ACKNOWLEDGMENTS

We are grateful to Drs. Kuriacose and Srinivasan of I. I. T. Madras, for providing the BET facilities. The authors also thank the Herdillia Chemicals Company for providing cumene for this work.

REFERENCES

1. Srivastava, R. K., and Srivastava, R. D., *J. Catal.* **39**, 317 (1975).
2. Varma, G. R., and Graydon, W. F., *J. Catal.* **28**, 236 (1973).
3. Verugdenhill, A. D., *J. Catal.* **28**, 493 (1973).
4. Casemier, J. H. R., Nieuwenhuys, B. E., and Sachtler, W. M. H., *J. Catal.* **29**, 367 (1973).
5. Norikoy, Y. D., and Smirnova, A. L., *Izu. Akad. Nauk SSSR, Ser. Khim.* **12**, 2688 (1974); *Chem. Abst.* **82**, 8579f (1975).
6. Kest, M. V., Evmenenko, N. P., and Gorokhovalskii, Y. B., *Katal. Katal.* **10**, 34 (1973).
7. Jacono, M., Schiavell, M., and Cimino, A., *J. Phys. Chem.* **75**, 1044 (1971).
8. Ermolenko, M. F., and Efros, M. D., *Zh. Fiz. Khim.* **38**, 1353 (1964).

9. Lafer, L. I., and Yakerson, V. I., *Izu. Akad. Nauk SSSR* **7**, 1448 (1971).

10. Swift, H. B., Lutinski, F. E., and Tobin, H. H., *J. Catal.* **5**, 285 (1966).

11. Wolfs, M. W. J., and Batist, Ph. A., *J. Catal.* **32**, 25 (1974).

12. Feller, M., and Field, E., U. S. Patent 2,880,200 (1959).

13. Stumpf, A., Russell, A. S., Newsome, J. W., and Tucker, C. M., *Ind. Eng. Chem.* **42**, 1398 (1950).

14. Sleight, A. W., and Chamberland, B. L., *Inorg. Chem.* **7**, 1672 (1968).

15. Giordano, N., Bart, J. C. J., Vaghi, A., Castellan, A., and Martinotti, G., *J. Catal.* **36**, 81 (1975).

16. Ferraro, J. R., "Low-Frequency Vibrations of Inorganic and Coordination Compounds." Plenum Press, New York, 1971.

17. Meyer, C., Clement, G., and Balaceanu, J. C., *Proc. Int. Congr. Catal., 3rd, 1964*, **1**, 184 (1965).

18. Neuberg, H. J., Phillips, M. J., and Graydon, W. F., *J. Catal.* **38**, 33 (1975).

19. Mukherjee, A., and Graydon, W. F., *J. Phys. Chem.* **71**, 4232 (1967).

20. Kamiya, Y., Beaton, S., Lafortune, A., and Ingold, K. U., *Canad. J. Chem.* **41**, 2034 (1963).

21. Tobolsky, A. V., Metz, D. J., and Mesrobian, R. B., *J. Amer. Chem. Soc.* **72**, 1942 (1950).

22. Schwab, G. M., *Z. Phys. Chem.* **25**, 411 (1934).